Paper No.
C2024-20887

AMPP ANNUAL CONFERENCE + EXPO
MARCH 3-7, 2024 | NEW ORLEANS, LOUISIANA

A disposable electrochemical biofilm/MIC test kit to detect MIC and to assess efficacy of biocide treatment of biofilm

Lingjun Xu
Dept. of Chemical & Biomolecular Eng.
Inst. for Corrosion & Multiphase Tech.
Ohio University
Athens, OH 45701, USA

Sith Kumseranee, Suchada Punpruk, Pruch Kijkla
PTTEP
Chatuchak, Bangkok 10900, Thailand

Adnan Khan
Dept. of Biological Sciences
Ohio University
Athens, OH 45701, USA

Tingyue Gu (gu@ohio.edu)
Dept. of Chemical & Biomolecular Eng.
Inst. for Corrosion & Multiphase Tech.
Ohio University
Athens, OH 45701, USA

ABSTRACT

Microbial biofilms are behind microbiologically influenced corrosion (MIC). Currently, all the so-called MIC test kits on the market are actually microbe test kits. Our new disposable miniature electrochemical biofilm/MIC test kit based on 10 ml serum vials with solid-state electrodes fills the gap to provide corrosion information such as abiotic corrosion vs. MIC, and MIC by electron-harvesting biofilms vs. MIC by corrosive metabolites. It can also test antimicrobial efficacy. An electrochemical workstation is used as a base station to perform various electrochemical scans such as linear polarization resistance, electrochemical impedance spectrometry and potentiodynamic polarization scans to provide near-real time transient corrosion data after a fluid or sludge is injected into the vial. This work presented a prototype with two different solid-state electrode choices. Three different methods to distinguish MIC from abiotic corrosion, and two different methods to distinguish MIC by electron-harvesting biofilms from MIC by corrosive metabolites. Anaerobic *Desulfovibrio ferrophilus* IS5 (a highly corrosive sulfate reducing bacterium) biofilm, aerobic *Pseudomonas aeruginosa* biofilm and an anaerobic corrosive oilfield biofilm consortium were used as examples. Tetrakis hydroxymethyl phosphonium sulfate (THPS) biocide was used as an example for assessing biocide efficacy. The patent-pending technology is currently undergoing field-testing.

Key words: *Biofilm sensor, biofilm kit, corrosion sensor, MIC, biocide efficacy*

INTRODUCTION

Corrosion has been a major issue in many industries, especially the oil and gas industry[1–3]. Nearly 25% of failures encountered in oilfields can be attributed to corrosion[4]. CO_2 corrosion and acid corrosion are common types of abiotic corrosion. CO_2 corrosion, also known as sweet corrosion or acid gas corrosion, of carbon steel has been extensively studied with the aim of reducing damage economic losses[5,6].

Microbiologically influenced corrosion (MIC) is an important branch in corrosion. Various microorganisms such as bacteria, archaea, fungi, and microalgae can cause MIC through their metabolic activities or metabolites[7–9]. Among them, sulfate reducing bacteria (SRB) are notorious and most prevalent for causing the most aggressive MIC[10,11]. Other bacteria such as nitrate reducing bacteria (NRB) were also found to be corrosive against carbon steels, stainless steels[12,13].

When SRB utilize extracellular electrons from Fe^0 oxidation for sulfate reduction, the electrons are transported from outside the SRB cells to the cytoplasm with the help of biofilm extracellular electron transfer (EET)[14]. This kind of MIC is known as EET-MIC (extracellular electron transfer-MIC)[15],

Extracellular: $4Fe \rightarrow 4Fe^{2+} + 8e^-$ ($E° = -447\ mV_{SHE}$) (1)

Intracellular: $SO_4^{2-} + 9H^+ + 8e^- \rightarrow HS^- + 4H_2O$ ($E°' = -217\ mV_{SHE}$) (2)

SRB can also corrode via M-MIC (metabolite-MIC), mainly because of the highly reactive sulfides. SRB MIC of Fe(0) at circumneutral pH is not caused by sulfides as demonstrated before[16]. However, this is not the case for SRB MIC of Cu. Cu is not energetic enough to supply electrons directly for sulfate reduction. However, H_2S can corrode Cu with H^+ as the electron acceptor, because the corrosion product Cu_2S is extremely insoluble[17,18].This makes the following corrosion reaction's Gibbs free energy change rather negative,

$$2Cu + HS^- + H^+ \rightarrow Cu_2S + H_{2(g)} \qquad (\Delta G°' = -58.3\ kJ/mol) \qquad (3)$$

In this case, H^+ at neutral pH becomes a feasible electron acceptor (oxidant) in Cu corrosion because the corrosion product Cu_2S has an extremely low solubility[19].

Riboflavin (RF) and magnetite nanoparticles (MNPs) are electron mediators that can accelerate EET[18,20]. They have been used to accelerate EET in *Desulfovibrio vulgaris* MIC of carbon steel. Thus, they are used to distinguish EET-MIC from M-MIC such as SRB MIC of Cu[18,21]. They can also be used to distinguish EET-MIC from abiotic corrosion, because the latter does not rely on cross-cell wall electron transfer (i.e., EET).

The most popular approach to mitigate MIC is biofilm mitigation mainly by using biocides and scrubbing (e.g., pigging)[22]. A biocide typically has no impact on abiotic corrosion unless the biocide chemical has non-biocidal functions. Therefore, biocide addition can potentially distinguish abiotic corrosion from biotic corrosion. THPS (tetrakis hydroxymethyl phosphonium sulfate) is known as a broad-spectrum biocide widely used in the field and in lab tests[23,24].

There is a third way to distinguish MIC from abiotic corrosion based on the fact that a living biofilm is behind MIC, and it responds to electrochemical tests in a special way. Tafel scan is a popular tool for both

abiotic and biotic corrosion research[25–27]. The orthodox Tafel scan method involves separate scans of the anodic and cathodic curves, which are performed on two replicate working electrodes (WEs) Each scan starts from the open circuit potential (OCP) (i.e., zero external voltage), extending to −200 mV (cathodic) vs. OCP and to +200 mV (anodic) vs. OCP (or higher if stainless steel passive film failure needs to be detected). To minimize the need for WEs in MIC, it is a common practice to scan continuously from the most negative potential to the most positive potential on a single WE, which is known as continuous upward scan. However, continuous upward scans in MIC introduce considerable distortions which often manifest as compression in the cathodic region and elongation in the anodic region (in voltage ranges), accompanied by a large deviation (typically around 50%) in corrosion current density (i_{corr}) compared to the orthodox scans. These distortions and i_{corr} deviation are attributed to insufficient time for a biofilm on the WE to adapt to the extreme externally-applied voltage (usually −200 mV vs. OCP)[28]. In comparison, the orthodox scan method, which starts each scan from OCP (i.e., no external voltage), allows time for the biofilm to adapt while the continuous upward scan method does not. It was found that even with the same WE, repeated half-scans starting from OCP did not cause large Tafel curve distortions and i_{corr} deviations[28]. Because an abiotic WE (no living biofilm involved) is far less prone to Tafel scan distortions and i_{corr} deviation using continuous upward scan method, the continuous upward scan comparison with dual-half scans can be used to distinguish abiotic corrosion from MIC.

In corrosion studies, weight loss and pitting rates are direct evidence for corrosion severity. Hanging coupons are placed inside pipelines or storage tanks to obtain weight loss and pitting data in field operations. Electrochemical tests such as LPR (linear polarization resistance) and Tafel scans are also widely used as a powerful tool to verify coupon weight loss results, especially in lab tests. EIS (electrochemical impedance spectroscopy) scans can provide additional information about charge transfer and mass transfer in the MIC process[29,30]. In various MIC studies, electrochemical test results were consistently found to support weight loss results[31–34]. Electrochemical data were also used in biocide efficacy studies and found to be consistent with weight loss reduction and sessile cell reduction trends[35,36]. The percentage in the reduction of i_{corr} or increase in R_p (polarization resistance from LPR) can be used as biocide efficacy or corrosion inhibition efficiency, and compared with weight loss-based and sessile cell reduction-based efficacies[36]. Among these electrochemical scans, LPR takes the least amount of time (e.g., as short as 2 min). Compared to coupon tests which only give cumulative results at the end of the corrosion period, electrochemical tests provide transient corrosion data. Therefore, the application of electrochemical tests makes near real-time corrosion rate measurements possible. For electrochemical tests, a typical 3E (3-electrode) setup consists of a WE (working electrode), a CE (counter electrode), and an independent (i.e., dedicated) RE (reference electrode). A typical RE needs an electrolyte solution, which makes it not suitable for a robust disposable MIC sensor. Thus, it is desirable to develop a solid-state RE. To simplify an MIC(/biofilm) test kit, a proper CE electrode can be chosen to serve as both CE and a pseudo-RE (p-RE) so the kit only has two connectors with the other connector being WE.

In this work, a disposable MIC test kit was presented for field applications which contains two solid-state electrodes. It is based on a common 10 mL serum vial for the injection of 5 mL to 7 mL of a field sample fluid or sludge to grow a biofilm on the WE surface. By using electrochemical scans employing a desktop or a battery-powered portable potentiostat, this MIC test kit can provide near real-time corrosion rate results and biocide efficacy data. Abiotic corrosion can be differentiated from biotic corrosion using one of the three different methods, and EET-MIC can be differentiated from M-MIC using electron mediators.

EXPERIMENTAL PROCEDURE

2. Materials and Methods

2.1 Bacteria, chemicals, and metals

Desulfovibrio ferrophilus (IS5 strain, DSM 15579) and an oilfield consortium (Consortium IIe) were grown in EASW (enriched artificial seawater) culture medium at 28 ºC and 37 ºC, respectively under anaerobic conditions. *Pseudomonas aeruginosa* was cultured aerobically in LB (Luria-Bertani) medium at 37 ºC, respectively. The pH of each medium was adjusted to 7.0 using HCl (5% w/w) and/or NaOH solution (5%) before autoclave sterilization. EASW was sparged with filter-sterilized N_2 gas for 1 h for deoxygenation. L-cysteine was then added as an oxygen scavenger at 20 ppm (w/w) in the culture medium in an anaerobic chamber filled with N_2.

The composition (g/L) of EASW was: Na_2SO_4 3.917, NaCl 23.476, $NaHCO_3$ 0.192, KBr 0.096, KCl 0.664, H_3BO_3 0.026, $SrCl_2{\cdot}6H_2O$ 0.040, $MgCl_2{\cdot}6H_2O$ 10.610, $CaCl_2{\cdot}2H_2O$ 1.469, yeast extract 1.0, tri-sodium citrate ($Na_3C_6H_5O_7$) 0.5, sodium lactate ($C_3H_5NaO_3$) 3.5, $CaSO_4{\cdot}0.5H_2O$ 0.1, NH_4Cl 0.1, $MgSO_4{\cdot}7H_2O$ 0.71, $Fe(NH_4)_2(SO_4)_2{\cdot}6H_2O$ 1.38, K_2HPO_4 0.05. The LB medium consisted of 10 g tryptone, 5 g yeast extract, 5 g NaCl, and in 1 L deionized water.

X65 carbon steel, 304 stainless steel (SS) and Cu (copper) (99.9% mass purity) were used in this work. Table 1 shows elemental compositions of X65 carbon steel and 304 SS. All metal coupons for WEs were polished to 600 grit. Anhydrous isopropanol (99% by volume) was used to sanitize electrode surfaces. Two different solid-state materials (code-named materials A and B) were tested as CE/p-RE.

Table 1. Elemental compositions (wt. %) of X65 and 304 SS (Fe balance).

Metal	C	Mn	P	N	Cr	S	Mo	Si	Ni	V	Nb	Co	Ti	Cu
X65	0.16	1.65	0.02			0.01		0.45		0.09	0.05		0.06	
304 SS		1.82		0.063	18.2		0.34	0.31	8.18			0.16		0.67

2.2 MIC test kit setup

The 10 mL MIC test kit consisted of a metal WE (1 cm^2 square work surface) and a solid-state CE/p-RE in a 10 mL anaerobic vial to form a disposable mini electrochemical glass cell (Fig. 1). For anaerobic tests, the vials were sealed with a rubber septum and aluminum cap. Silicone glue was used to seal the cap as an extra measure against possible gas leak. Sample liquids were injected into the MIC test kit with a needle.

Fig. 1. (A) Multiple units of 10 mL biofilm/MIC test kit to be shipped out for field testing with electrochemical scans that can be performed using a battery-powered portable potentiostat (cell phone with app for it shown on top), (B) test kit setup for abiotic and (C) biotic tests with X65 WE and a solid-state material as CE/p-RE.

2.3 Tafel scans

Tafel scans were performed on each 10 mL electrochemical glass cell at 3 d (time needed to grow a mature biofilm on WE) of incubation at a scan rate of 0.167 mV/s. A PCI4/750 potentiostat (Gamry Instruments, Inc., Warminster, PA, USA) was used for measurements. Dual-half scans from 0 to −200 mV (vs. OCP) and 0 to +200 mV (vs. OCP) were followed by a continuous upward scan from −200 mV (vs. OCP) to +200 mV (vs. OCP) using the same 10 mL electrochemical glass cell.

2.4 Injection test

Injection tests were carried out at 3 d biofilm growth. LPR was scanned at a rate of 0.167 mV/s from the range of −10 to 10 mV vs. OCP every 20 min to get a stable R_p (polarization resistance) curve over 1 h. Then, RF or MNPs were injected into the cell to reach a final concentration of 20 ppm in the liquid. The vial was gently shaken for 3 min to disperse riboflavin or MNPs. LPR measurements were performed every 10 min to monitor R_p. After R_p became relatively stable for at least 30 min, THPS was injected to reach 100 ppm. The vial was again gently shaken for 3 min, and R_p was monitored every 10 min until it stabilized.

2.5 Biocide efficacy assessment

Biocide efficacy was assessed using the MIC test kit in both biofilm prevention and biofilm eradication tests. In the biofilm prevention test, a biocide was added before inoculation. LPR was scanned starting right after inoculation (0 d) to observe biofilm buildup impact on MIC and biocide inhibition of the biofilm and MIC. R_p was recorded during the 7-d incubation and compared to the control (no biocide treatment). In the biofilm eradication test, a biofilm was grown for 3 d. Then, a biocide was injected into the medium and R_p response to the injection was monitored. The stable R_p value after biocide injection was compared with the pre-injection R_p value for biocide efficacy estimation.

RESULTS AND DISCUSSION

Biofilm prevention test

In the biofilm prevention test, 50 ppm THPS was added upon *D. ferrophilus* inoculation into a MIC test kit vial containing X65 WE and material A CE/p-RE. Over the 7-d incubation period, the R_p of 50 ppm THPS vial was consistently higher than that of the no treatment control in Fig. 2, indicating lower corrosion throughout the incubation. In this case, the low 50 ppm dosage of THPS only delayed *D. ferrophilus* biofilm maturity by one day, but did not stop it (i.e., the biocide treated R_p did not stay flat on top). The no treatment curve (black) shows that biofilm corrosivity first peaked at 3 d while the 50 ppm THPS curve at 4 d. This test shows that the MIC test kit can be used as a tool to evaluate a biocide's biofilm prevention efficacy.

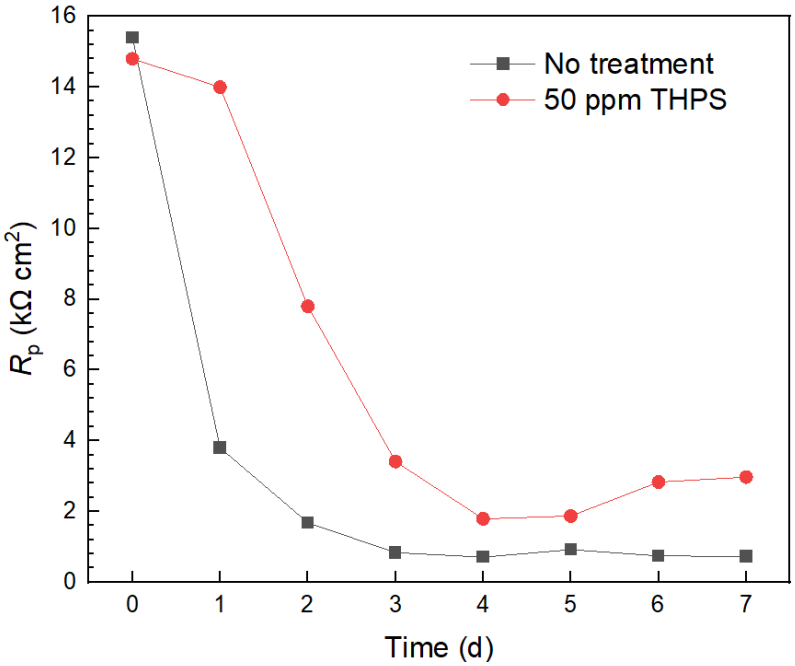

Fig. 2. R_p during 7-d incubation of *D. ferrophilus* with and without 50 ppm THPS in 10 mL MIC test kit consisting of X65 WEs and material A CEs/p-RE.

Tafel scan curves

In Fig. 3, in a 10 mL vial containing X65 WE and material B CE/p-RE with *D. ferrophilus* in 5 mL EASW, continuous upward scan from −200 mV to 200 mV (vs. OCP) at 3-d incubation reduced i_{corr} by 59% with compressed cathodic curve and elongated anodic curve compared to the rather symmetric curves from the dual-half scans that started from OCP. This pattern of Tafel skews in the 10 mL vial was similar to a previously reported case in a 3-electrode 450 mL full-size glass cell with C1018 carbon steel WE, platinum CE, SCE RE[28], although the y-axis voltage positions are different because the MIC test kit used a p-RE, rather than a dedicated reference electrode like SCE.

In abiotic CO_2 corrosion, the continuous upward scan resulted in a rather small i_{corr} reduction of only 11% compared to the dual-half scans using X65 WE and material B CE/p-RE at 2 d immersion in Fig. 4. Negligible compression of the cathodic curve and elongation of the anodic curve were observed for the continuous upward scan. The data above show that Tafel skews were pronounced in SRB MIC of carbon steel, but not so in abiotic CO_2 corrosion. Thus, Tafel skews (curve distortions and i_{corr} deviation) can be used to distinguish abiotic corrosion from MIC.

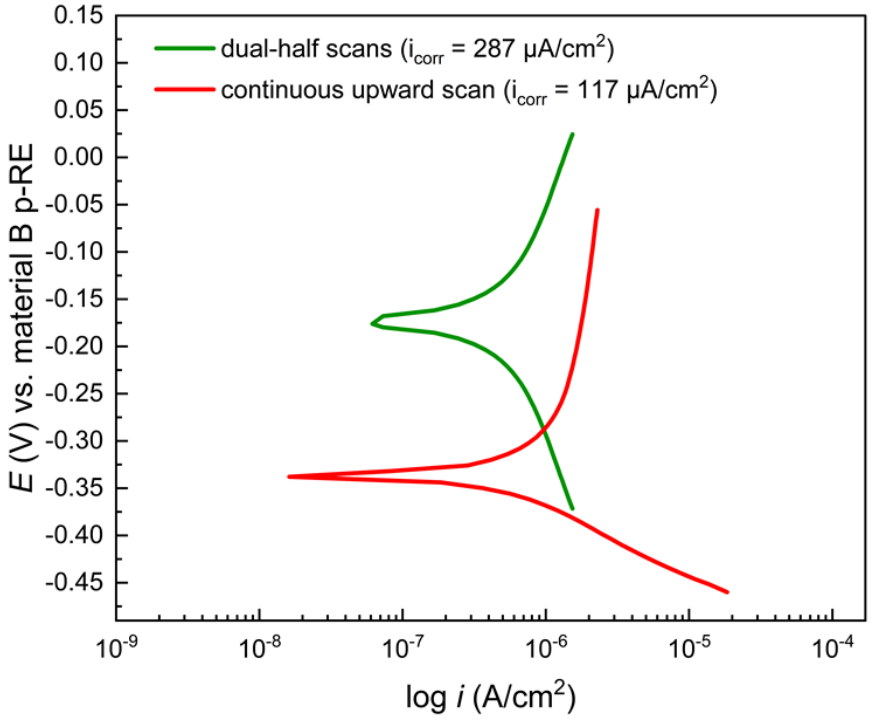

Fig. 3. Dual-half scans using X65 WE and material B CE/p-RE exhibiting rather “symmetric” anodic and cathodic curves compared to continuous upward scan in 10 mL MIC test kit with *D. ferrophilus* in EASW showing compression of cathodic curve and elongation of anodic curve with i_{corr} decrease of 59% in continuous upward scan.

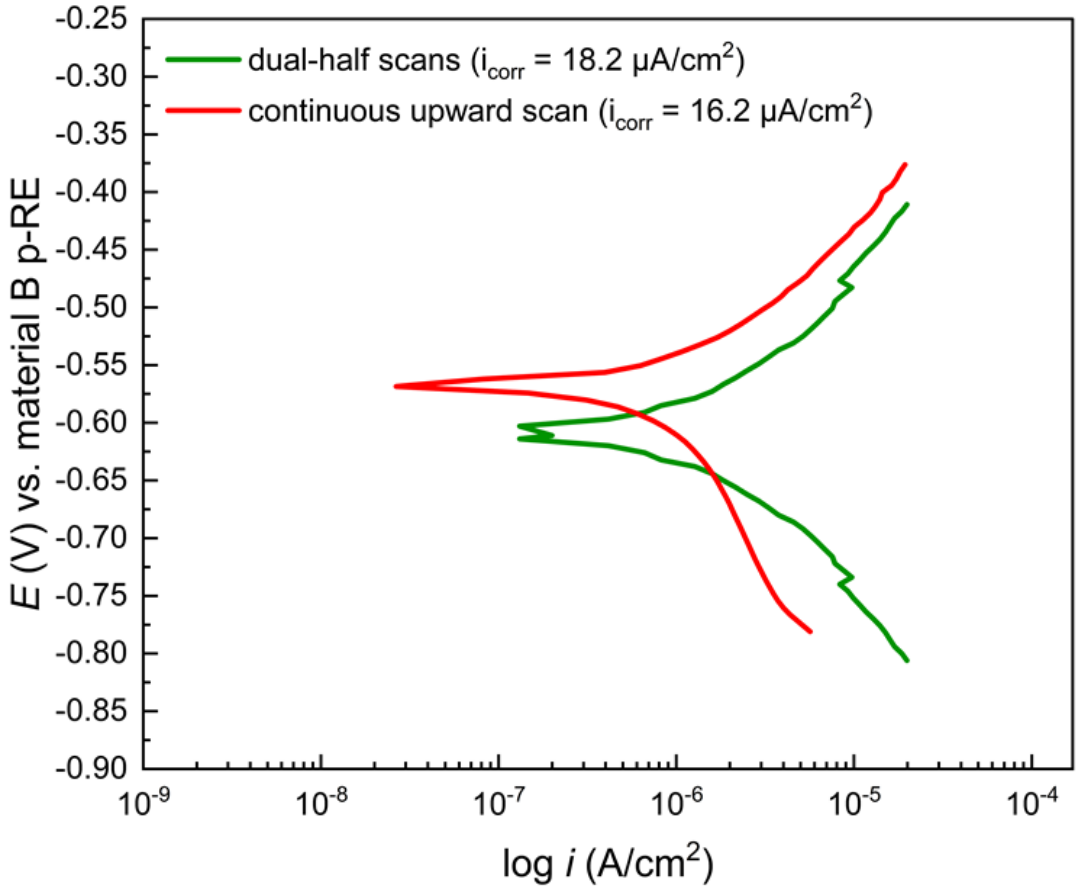

Fig. 4. Dual-half scans in a 10 mL vial with X65 WE and material B CE/p-RE exhibiting negligible Tafel skews and small i_{corr} decrease of 11% in continuous upward scan compared with dual-half scans, indicating abiotic corrosion.

Injections of electron mediator and biocide

Riboflavin electron mediator and THPS biocide were injected in tandem into 10 mL MIC test kits in different abiotic and biotic corrosion systems. In Fig. 5, after a 1 h stable R_p was achieved prior to injections at around 3 d, 20 ppm (final concentration in broth) riboflavin injection resulted in a disturbance in R_p. It was due to the disturbance of the background solution caused by the injection itself. After the disturbance, R_p quickly returned to the baseline level at 20 min (post-injection time mark) and remained stable for another 30 min, indicating no acceleration of the corrosion by riboflavin (i.e., R_p not decreased by riboflavin). This was because abiotic CO_2 corrosion did not involve EET. The subsequent THPS biocide injection elicited a similar response, indicating that THPS did not inhibit abiotic CO_2 corrosion, because the corrosion was not caused by a living biofilm.

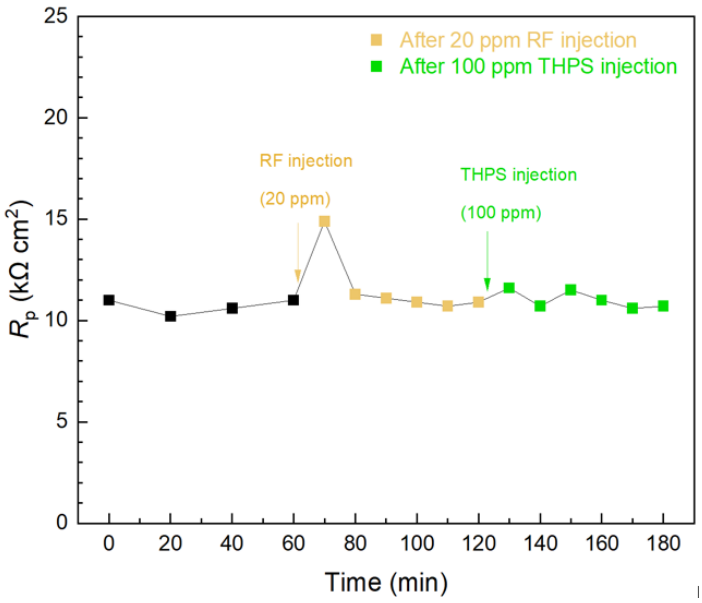

Fig. 5. Variations of R_p of X65 WE with material B CE/p-RE after 20 ppm riboflavin (RF) injection at 3 d followed by 100 ppm THPS injection in 10 mL MIC test kit containing 5% (w/w) NaCl solution sparged with CO_2 (pH 4).

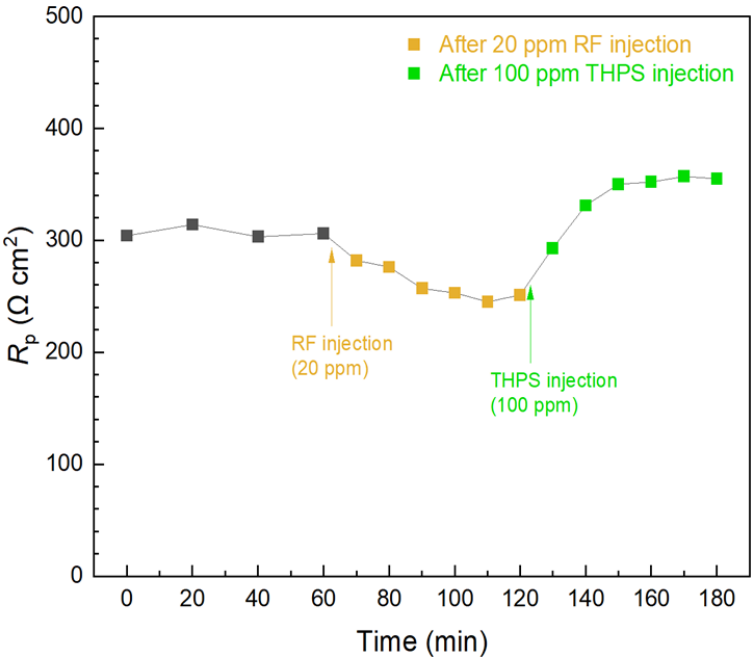

Fig. 6. Variations of R_p of X65 WE with material B CE/p-RE after 20 ppm riboflavin injection at 3 d followed by 100 ppm THPS injection in 10 mL MIC test kit with *D. ferrophilus* in EASW.

In comparison, riboflavin and THPS both considerably affected corrosion rate (reflected by $1/R_p$) in *D. ferrophilus* corrosion in Fig. 6. After the riboflavin injection at 3-d SRB incubation, R_p showed a decreasing trend and stabilized 1 h after injection. Compared with the pre-injection value, R_p decreased by 17%, indicating corrosion acceleration by this electron mediator as expected because SRB MIC of carbon steel belongs to EET-MIC[21]. In the same 10 mL vial, the subsequent THPS injection resulted in R_p increase by 41% within 1 h. This phenomenon was attributed to the biofilm kill by 100 ppm THPS, which increased

R_p and reduced the corrosion rate. In Fig. 7, another CE/p-RE material was used in *D. ferrophilus* corrosion. The R_p responses of X65 WEs to riboflavin and THPS injections were similar. The results indicate that different solid-state materials can be used as the CE/p-RE in the MIC test kit.

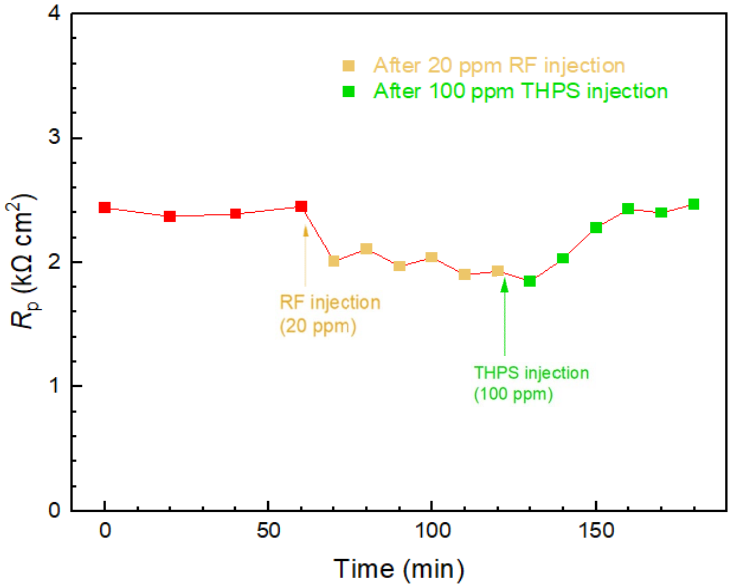

Fig. 7. Variations of R_p of X65 WE with material A CE/p-RE after 20 ppm riboflavin injection at 3-d incubation followed by 100 ppm THPS injection in 10 mL MIC test kit with *D. ferrophilus* in EASW.

Fig. 8 shows the result of THPS injection test without riboflavin injection. After the 100 ppm THPS injection, R_p increased by 42% within 0.5 h, which can be used as the R_p-based biocide treatment efficacy or corrosion inhibition efficiency[37].

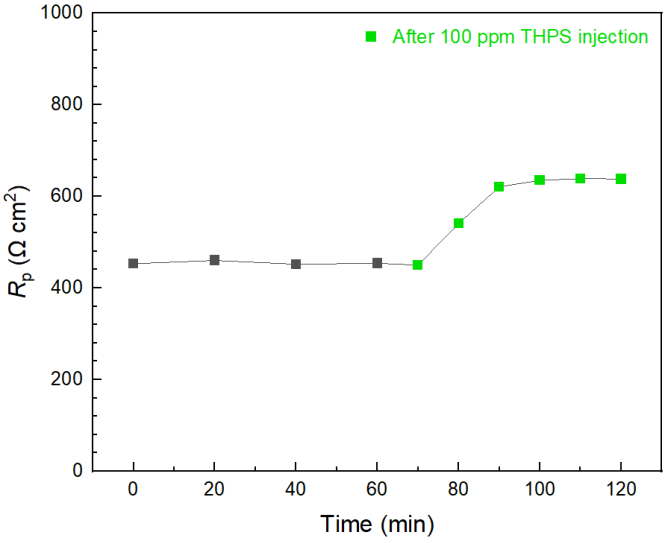

Fig. 8. Variations of R_p of X65 WE with material B CE/p-RE after 100 ppm THPS injection in 10 mL MIC test kit with *D. ferrophilus* in EASW.

Tandem injections of MNP, riboflavin and THPS were also conducted in a MIC test kit containing oilfield biofilm Consortium IIe which contained *D. vulgaris* and other microbes reported in a different study[38]. Fig. 9 indicates that MNPs injection (20 ppm in broth) decreased R_p, whereas the following 100 ppm THPS injection increased R_p. The subsequent tandem injections of 20 ppm riboflavin and 100 ppm THPS also resulted in decrease and increase in R_p, respectively which was consistent with electron mediator acceleration of SRB MIC of carbon steel and biocide mitigation of the MIC. Therefore, this MIC test kit is applicable to systems with a mixed culture biofilm in confirming biotic corrosion and EET-MIC.

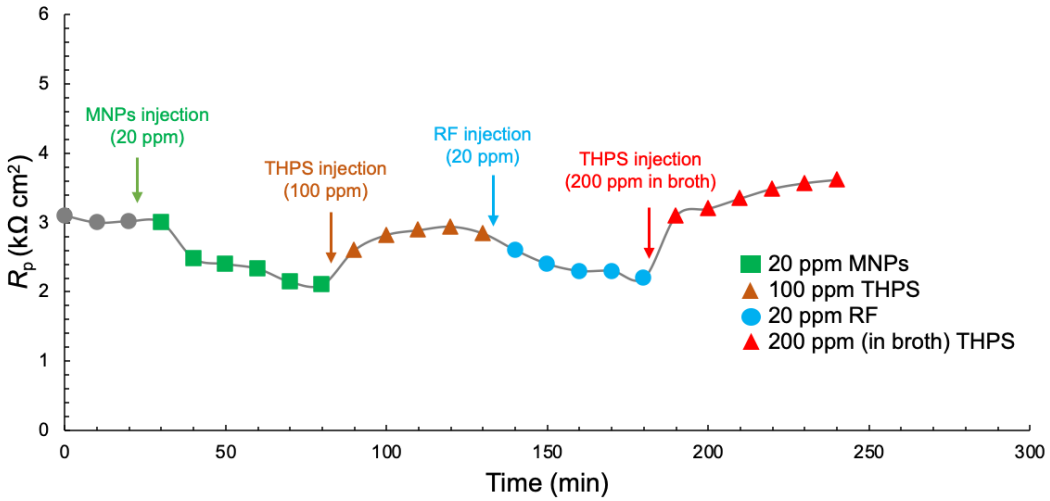

Fig. 9. R_p before and after tandem injections of electron mediators, namely, MNPs and riboflavin (RF), and biocide THPS at 3 d of incubation with Consortium CIIe in 10 mL MIC test kit containing X65 WE and material B CE/p-RE.

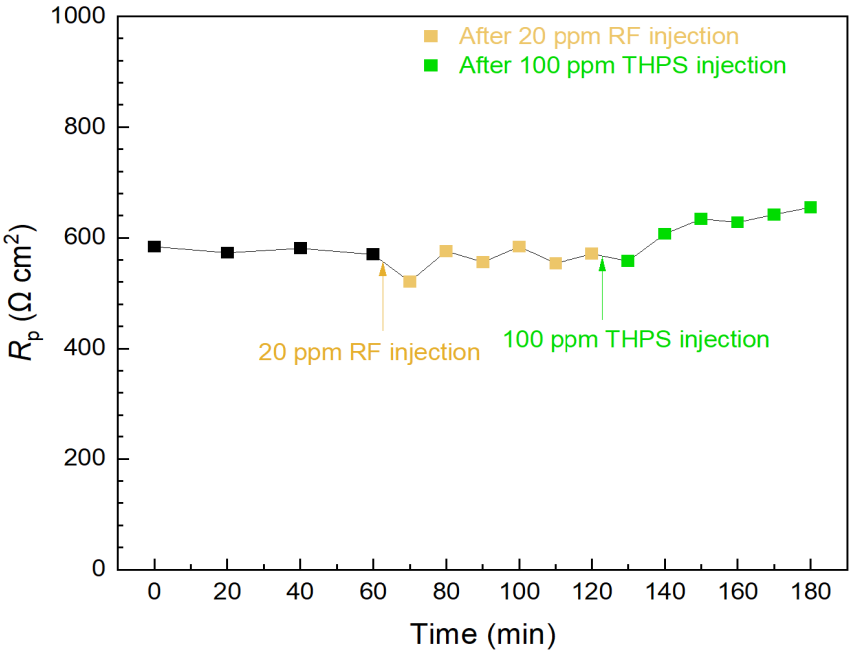

Fig. 10. R_p of Cu WE with material B CE/p-RE after 20 ppm riboflavin injection at 3-d incubation (showing no MIC acceleration for this biogenic H_2S M-MIC of Cu), followed by 100 ppm THPS injection in 10 mL MIC test kit incubated with *D. ferrophilus* in EASW.

When Cu was used as the WE for *D. ferrophilus* MIC, the 20 ppm riboflavin injection didn't cause significant changes in R_p in Fig. 10. This indicates that SRB MIC of Cu is not EET-MIC. It has been proven to be M-MIC as evidenced by increased H_2 evolution previously[18]. Therefore, riboflavin injection can be used as a tool to distinguish EET-MIC from M-MIC. The injection of 100 ppm THPS increased R_p by 15% which indicates biocide mitigation of Cu MIC by SRB and possible scavenging of H_2S by THPS. The increase in R_p caused by the biocide was not as high as that in EET-MIC systems which could be because in M-MIC, biofilm mitigation still left behind some corrosive metabolites.

Injection tests of riboflavin and THPS were also performed in aerobic *P. aeruginosa* MIC of 304 SS. It was known that the corrosion belongs to EET-MIC with O_2 as the terminal electron acceptor[39]. In Fig. 11, a 27% decline in R_p was observed after the 20 ppm riboflavin injection, whereas the following 100 THPS injection increased R_p by 33%. These results prove that the injection tests are useful in both anaerobic and aerobic MIC systems and can be used to distinguish abiotic corrosion from MIC, and EET-MIC from M-MIC.

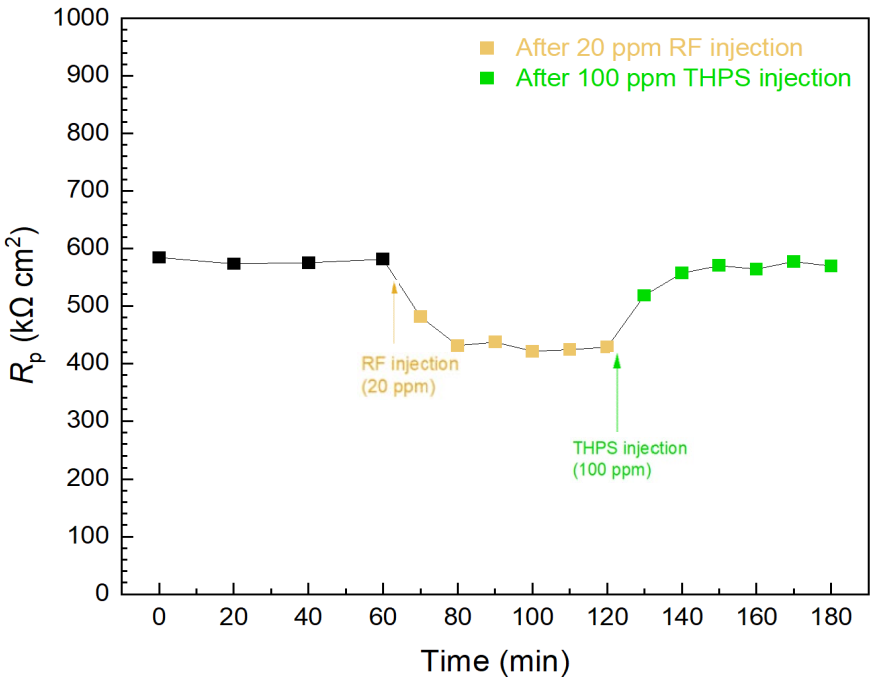

Fig. 11. R_p of 304 SS WE with material B CE/p-RE after 20 ppm riboflavin injection at 3-d incubation followed by 100 ppm THPS injection in 10 mL MIC test kit vial incubated with aerobic *P. aeruginosa* in LB culture medium.

CONCLUSIONS

The following conclusions can be drawn from the experimental data in this work:

- The biofilm/MIC test kit using a metal WE and a solid-state CE/p-RE in a 10 mL vial is disposable and easy to use. It can be used in different MIC systems as well as in abiotic corrosion.
- Different solid-state materials can serve as the CE/p-RE.

- Biocide efficacy or corrosion inhibition can be assessed through biofilm prevention test and biofilm eradication (i.e., injection) test using the MIC test kit.
- Three different methods can be used to distinguish abiotic corrosion from MIC.
- EET-MIC can be distinguished from M-MIC by using electron mediator riboflavin or MNPs.

ACKNOWLEDGEMENTS

We acknowledge the financial support from PTTEP and Petrobras.

REFERENCES

1. Xu, D., T. Gu, and D.R. Lovley, *Nat. Rev. Microbiol.* (2023): pp. 1–14. https://www.nature.com/articles/s41579-023-00920-3.
2. Engelhardt, G.R., R.C. Woollam, and D.D. Macdonald, *ECS Trans.* 50 (2013): p. 141.
3. Ropital, F., *Mater. Corros.* 60 (2009): pp. 495–500.
4. Ossai, C.I., *Int. Sch. Res. Not.* 2012 (2012).
5. Edmonds, D.V., and R.C. Cochrane, *Mater. Res.* 8 (2005): pp. 377–385.
6. Dugstad, A., “Fundamental Aspects of CO2 Metal Loss Corrosion, Part I: Mechanism” (2015), p. NACE-2015-5826.
7. Kiani Khouzani, M., A. Bahrami, A. Hosseini-Abari, M. Khandouzi, and P. Taheri, *Metals* 9 (2019): p. 459.
8. Beale, D.J., A.V. Karpe, S. Jadhav, T.H. Muster, and E.A. Palombo, *Corros. Rev.* 34 (2016): pp. 1–15.
9. Liu, X., Y. Qian, Y. Wang, F. Wu, W. Wang, and J.-D. Gu, *Curr. Opin. Biotechnol.* 75 (2022): p. 102716.
10. Cui, L., Z. Liu, P. Hu, and J. Shao, *J. Mater. Eng. Perform.* 30 (2021): pp. 7584–7596.
11. Fadzir, M.F.M., A.B.A. Bakar, and D.K.D. Kurniawan, *J. Mek.* (2015).
12. Liu, B., E. Fan, J. Jia, C. Du, Z. Liu, and X. Li, *Constr. Build. Mater.* 303 (2021): p. 124454.
13. Iino, T., K. Ito, S. Wakai, H. Tsurumaru, M. Ohkuma, and S. Harayama, *Appl. Environ. Microbiol.* 81 (2015): pp. 1839–1846.
14. Wan, H., T. Zhang, Z. Xu, Z. Rao, G. Zhang, G. Li, and H. Liu, *Corros. Sci.* 212 (2023): p. 110963.
15. Pu, Y., Y. Tian, S. Hou, W. Dou, and S. Chen, *Npj Mater. Degrad.* 7 (2023): p. 7.
16. Lv, M., and M. Du, *Rev. Environ. Sci. Biotechnol.* 17 (2018): pp. 431–446.
17. Han, F., W. Li, D. Li, and A. Lu, *ChemElectroChem* 1 (2014): pp. 733–740.
18. Wang, D., J. Liu, R. Jia, W. Dou, S. Kumseranee, S. Punpruk, X. Li, and T. Gu, *Corros. Sci.* 177 (2020): p. 108993.
19. Licht, S., *J. Electrochem. Soc.* 135 (1988): p. 2971.
20. Guan, F., Z. Liu, X. Dong, X. Zhai, B. Zhang, J. Duan, N. Wang, Y. Gao, L. Yang, and B. Hou, *Sci. Total Environ.* 788 (2021): p. 147573.
21. Wang, D., P. Kijkla, M.E. Mohamed, M.A. Saleh, S. Kumseranee, S. Punpruk, and T. Gu, *Bioelectrochemistry* 142 (2021): p. 107920.
22. Chugh, B., S. Thakur, and A.K. Singh, *Corros. Inhib. Oil Gas Ind.* (2020): pp. 321–338.
23. Conlette, O., *Br. Microbiol. Res. J.* 4 (2014): pp. 1463–1475.
24. Okoro, C.C., *Pet. Sci. Technol.* 33 (2015): pp. 1366–1372.
25. Kahyarian, A., B. Brown, and S. Nesic, *Corros. Sci.* 129 (2017): pp. 146–151.
26. Cetin, D., and M.L. Aksu, *Corros. Sci.* 51 (2009): pp. 1584–1588.
27. Shi, Z., M. Liu, and A. Atrens, *Corros. Sci.* 52 (2010): pp. 579–588.
28. Wang, D., P. Kijkla, M.A. Saleh, S. Kumseranee, S. Punpruk, and T. Gu, *J. Mater. Sci. Technol.* 130 (2022): pp. 193–197.

29. Juzeliūnas, E., R. Ramanauskas, A. Lugauskas, M. Samulevičienė, and K. Leinartas, *Electrochem. Commun.* 7 (2005): pp. 305–311.
30. Moreno, D., J. Ibars, J. Polo, and J. Bastidas, *J. Solid State Electrochem.* 18 (2014): pp. 377–388.
31. Liu, H., C. Chen, X. Yuan, Y. Tan, G. Meng, H. Liu, and Y.F. Cheng, *Corros. Sci.* 203 (2022): p. 110345.
32. Liu, H., and Y.F. Cheng, *Corros. Sci.* 173 (2020): p. 108753.
33. Liu, H., Y.F. Cheng, D. Xu, and H. Liu, *J. Electrochem. Soc.* 165 (2018): p. C354.
34. Liu, H., and Y.F. Cheng, *Corros. Sci.* 133 (2018): pp. 178–189.
35. Abbas, M.A., K. Zakaria, A.M. El-Shamy, and S.Z.E. Abedin, *Z. Für Phys. Chem.* 235 (2021): pp. 377–406.
36. Wang, J., H. Liu, M.E.-S. Mohamed, M.A. Saleh, and T. Gu, *J. Mater. Sci. Technol.* 107 (2022): pp. 43–51.
37. Morad, M., *Corros. Sci.* 50 (2008): pp. 436–448.
38. Li, Y., R. Jia, H.H. Al-Mahamedh, D. Xu, and T. Gu, *Front. Microbiol.* 7 (2016): p. 896.
39. Huang, Y., E. Zhou, C. Jiang, R. Jia, S. Liu, D. Xu, T. Gu, and F. Wang, *Electrochem. Commun.* 94 (2018): pp. 9–13.